Applications of a Multiple Linear Regression Model to the Analysis of Relationships between Eastward- and Westward-Moving Intraseasonal Modes

PAUL E. ROUNDY

NOAA–CIRES Aeronomy Laboratory, Boulder, Colorado

WILLIAM M. FRANK

Department of Meteorology, The Pennsylvania State University, University Park, Pennsylvania

(Manuscript received 13 February 2004, in final form 14 June 2004)

ABSTRACT

Multiple linear regression models with nonlinear power terms may be applied to find relationships between interacting wave modes that may be characterized by different frequencies. Such regression techniques have been explored in other disciplines, but they have not been used in the analysis of atmospheric circulations. In this study, such a model is developed to predict anomalies of westward-moving intraseasonal precipitable water by utilizing the first through fourth powers of a time series of outgoing longwave radiation that is filtered for eastward propagation and for the temporal and spatial scales of the tropical intraseasonal oscillations. An independent and simpler compositing method is applied to show that the results of this multiple linear regression model provide a better description of the actual relationships between eastward- and westward-moving intraseasonal modes than a regression model that includes only the linear predictor.

A statistical significance test is applied to the coefficients of the multiple linear regression model, and they are found to be significant over broad regions of the Tropics. Correlations between the predictors are shown to not significantly influence results for this case.

Results show that this regression model reveals physical relationships between eastward- and westward-moving intraseasonal modes. The physical interpretation of these regression relationships is given in a companion paper.

1. Introduction

It is widely accepted that two different processes that are characterized by different frequencies may interact constructively or destructively with one another even though they are not linearly correlated. Some atmospheric examples of such interactions include the tropical Madden–Julian, or intraseasonal, oscillation (ISO; Madden and Julian 1994) interacting with the El Niño–Southern Oscillation (ENSO; e.g., Kessler and Kleeman 2000) and higher-frequency equatorial waves interacting with the ISO (e.g., Dickinson and Molinari 2002; Straub and Kiladis 2003). The effects of these interactions are often directed both from lower to higher frequencies and vice versa. For example, the interannual ENSO modulates the geographical locations where the intraseasonal ISO produces high-amplitude convective anomalies over the Pacific Ocean (Kessler 2001), and the ISO can modulate oceanic Kelvin wave activity, which may be a precursor of lower-frequency warm ENSO events (e.g., Hendon et al. 1998). Because such interacting processes may not be linearly correlated, linear statistics alone cannot always be applied directly to assess the nature of the interactions.

In a companion paper, Roundy and Frank (2004b, hereafter RF) discuss systematic interactions between eastward- and westward-moving intraseasonal modes (labeled here ISOe and ISOw, respectively). They do this by applying a multiple linear polynomial regression model that includes the first through fourth powers of a time series index of the ISOe as predictors of fields of data. The data fields include outgoing longwave radiation (OLR) and precipitable water (PW) anomaly data filtered in wavenumber and frequency for two bands representing the ISOe and the ISOw.

Their results (especially their Figs. 1, 3, and 4) indicate that eastward- and westward-propagating intraseasonal modes cooperatively interact with each other to help produce many of the characteristics of the observed ISO. They also find that the ISOe and the ISOw modes excite or amplify one another through interactions facilitated by land and/or convection. They further show that ISOw convective anomalies amplify (weaken) as they propagate through regions of active (suppressed) ISOe convection and that the interactions tend to pro-

Corresponding author address: Paul Roundy, NOAA–CIRES Aeronomy Laboratory, R/AL3, 325 Broadway, Boulder, CO 80305-3328. E-mail: proundy@al.noaa.gov

duce standing oscillation patterns in some regions. The related westward-moving modes are often characterized by somewhat higher frequencies than are the eastward-moving modes, so a linear regression model with only a linear predictor cannot diagnose the entire relationship.

The regression method applied by RF has not been widely used in meteorology, but it has proven useful in other disciplines (e.g., biology, Sokal and Rohlf 1995). The purpose of the current paper is to describe how this technique can be applied to the study of atmospheric waves and to show that the use of this technique produces new and potentially interesting results that are truly descriptive of atmospheric processes. The current paper demonstrates that the application of the nonlinear terms is both valid and useful in revealing physical relationships. We support this argument by comparing the results to those of a much simpler compositing technique. This paper also discusses a statistical analysis of the model itself, including a statistical significance test applied to the coefficients.

In some applications of similar models, linear correlations between predictors may distort or otherwise invalidate the model results. We show that such correlations do not significantly influence results in our application of the model. We leave the physical interpretation of the regression model results to the companion paper.

2. Data and model description

a. Data

Data relevant to this part of the project include OLR and PW. Interpolated OLR data [from the National Oceanic and Atmospheric Administration (NOAA) near-polar-orbiting satellites] were acquired from the Climate Diagnostics Center (CDC) on a 2.5° grid (Liebmann and Smith 1996). The NASA Water Vapor Project (NVAP) provided daily PW data on a 1° grid (Randel et al. 1996). The PW data were interpolated to a 2.5° grid, then both OLR and PW were filtered for eastward- and westward-propagation in intraseasonal frequencies [including one band for the ISOe (wavenumbers 0–6 eastward and periods of 26–104 days) and another for the ISOw (wavenumbers 1–6 westward and periods of 15–104 days)] as described by RF. Both filter bands isolate similar frequencies and wavenumbers such that they include the eastward- and westward-moving components of any standing behavior. The ISOe filter does not include the 15–26-day band to avoid the signal of the potentially unrelated convectively coupled Kelvin wave (Wheeler and Kiladis 1999), as discussed by RF. Wheeler and Kiladis (1999) designed a filter to isolate $n = 1$ ER waves in the broad ISOw region. Their filter extends to somewhat higher frequencies and wavenumbers than does our ISOw filter, but their filter does not enclose a region of significant power in the lower frequencies of the ISOw region (see their Fig. 6). These lower frequencies are included in the ISOw filter because of their potential connection to the ISOe.

b. The linear regression model with nonlinear terms

The polynomial regression model is

$$y_{s,t+\tau} = a_{0,s,\tau} + a_{1,s,\tau}x_t^1 + a_{2,s,\tau}x_t^2 + a_{3,s,\tau}x_t^3 + a_{4,s,\tau}x_t^4 + \varepsilon_{s,\tau}, \quad (1)$$

where y is the modeled variable (in the current paper y is ISOw band PW) and x is the predictor variable (ISOe band-filtered OLR at 10°S, 90°E including only wavenumbers 1–4 and 26–104-day periods). The filter for the base index contains a smaller range of wavenumbers than the ISOe filter discussed above to ensure that its signal is dominated by the signal of the large-scale components of the MJO (Wheeler and Kiladis 1999). The location of the base point at 10°S, 90°E was selected because it is near the point of maximum variance of the ISOe band OLR during the southern summer. Use of this point allows the composite to diagnose patterns that occur during the southern summer because only periods when the base index is active are included in the regression and because the meridional structure of the ISOe varies seasonally (see RF). The term ε represents the model residuals, τ represents a time lag, and s represents the spatial coordinate. The a_n coefficients are regression parameters that are determined by a simple matrix operation, as follows. After ignoring the residuals, Eq. (3) may be written in matrix form (Wilks 1995):

$$\mathbf{y}_{s,t+\tau} = \mathbf{X}_t\mathbf{a}_{s,\tau}. \quad (2)$$

This may be solved at a given lag for the vector of regression coefficients (**a**):

$$\mathbf{a}_{s,\tau} = (\mathbf{X}_t^T\mathbf{X}_t)^{-1}\mathbf{X}_t^T Y_{s,t+\tau}, \quad (3)$$

where superscript T represents the matrix transpose. Composites are generated by calculating the coefficients **a** at each grid point s and over a range of τ, followed by substituting an arbitrary value for x, which we chose to be two standard deviations below the mean of the index series (e.g., Hendon and Salby 1994; Wheeler et al. 2000).

c. Motivation

Inclusion of such higher-power terms is not a new idea (Wilks 1995; Draper and Smith 1966). Wilks notes that this method of applying higher powers of predictors as additional predictors is generally acceptable and often results in a better statistical model for the relationship between two variables. He states that addition of such terms may be motivated by physical reasons or simply by suggestion of nonlinear relationships from examination of a scatterplot. We argue that a power series of

a single predictor can be applied in a linear model framework to extract many functional physical relationships between two variables, and it provides a model analogous in some respects to a Taylor series approximation of the true relationship.

Our primary motivation for including the higher-order terms is that they improve the model fit between the base-point OLR and the gridpoint ISOw band PW data, discussed below. There is also some physical motivation for applying higher-order terms. The frequencies of many of the waves that occur in the ISOw band and are related to the ISOe are not necessarily always the same as those of the ISOe disturbances themselves. The scales and frequencies of the ISOw waves change due to accelerations as they propagate from regions that do not support deep convection into regions that do support convection and as they propagate through varying background wind states including different phases of the ISOe. In general, our results reveal that ISOw waves that are linked to the ISOe tend to be characterized by frequencies the same as or higher than those of their ISOe counterparts. The phase accelerations result in local changes in frequency, which reduce the effectiveness of the linear term because linear correlations are not retained when the frequency changes. Lack of linear correlation causes the regressed anomalies to disappear from a fully linear model in the regions where such accelerations occur, even though the anomalies that the regressions are intended to diagnose may actually be continuous. Use of the nonlinear terms reclaims much of the lost signal.

The dominant frequencies in the ISOw band are two to three times those of the ISOe band (e.g., the spectra of Wheeler and Kiladis 1999). This leaves open the possibility that ISOw waves may be more coherent with higher powers of the ISOe than they are with its first power at many locations. Because the base-point data fluctuates like a wave, its higher powers are characterized by frequencies that are higher than the frequencies in the original data. For example, the square of a sine wave of frequency f has a frequency equal to 2f. Equation (1) is therefore most useful if the time series for x is characterized by a range of frequencies that are equal to or lower than those that characterize the time series for y, making this model especially useful for finding relationships between the ISOe and the ISOw. Further discussion of the physical interpretation of the higher-power terms is given in sections 4b,c.

3. Methodology

Independent verification of regression model

The companion paper (RF) analyzes interactions between ISOe and ISOw anomalies using the regression model described above. Their Fig. 1 shows their composite analysis of these interactions in the longitude–time lag domain. In the current paper we wish to demonstrate that the regression model of RF produces results that are representative of physical processes. We do this by comparing the results of the RF regression composite analysis to results from a fully linear analysis and to an independent composite analysis that does not involve use of a regression model.

The independent composite of westward-moving anomalies was calculated by simply selecting a set of dates when peaks of high amplitude ISOe negative OLR anomalies occurred at a base point and by averaging the ISOw bandpass-filtered PW over lags from those dates. The base point chosen was the same one used in RF (10°S and 90°E), where the ISOe band OLR tends to be most active during the southern summer. (Further discussion of this base point and the associated time series is given by RF.) We eliminated any time periods in the index ISOe series when the signal was not deemed to be present. The signal was assumed to not be present if a 61-day-centered window segment of the series had a lower variance than the variance of the entire series (e.g., Hendon and Salby 1994; Wheeler et al. 2000). We then found the dates when the absolute value of the time derivative of the index series was less than a threshold. These dates correspond approximately to the times of local extrema in the OLR series. The threshold we selected was 0.35 W m^{-2} day^{-1}. It was adjusted to give a large sample size while including most extrema only once. A smaller threshold results in a smaller sample size because the data are discrete, whereas a larger threshold tends to include multiple observations at different times on the same anomalies, resulting in a more washed-out signal far from the base point and the zero lag. In addition to the near-zero derivative, the amplitude was required to be less than two standard deviations below the mean (e.g., Hendon and Salby 1994). This amplitude threshold helps to select the dates of the minima of a set of strong negative OLR anomalies from among the dates of local extrema selected by applying the time derivative threshold. The ISOw bandpass-filtered PW at each grid point was then averaged for a set of lags of -75 to $+75$ days from the set of dates selected from the index series.

4. Results

a. Comparison of the three composites

The results of the fully linear model, the independent composite average, and the model that includes the three nonlinear terms are given in Figs. 1a–c, respectively. These diagrams are formatted similarly to Fig. 3b of RF. Each panel is a longitude–time lag representation of regressed or composited ISOw PW anomalies that are averaged from 2.5° to 7.5°N. In the companion paper, RF explains the purpose of this averaging, which is that anomalies produced by westward-moving ER waves tend to have higher amplitudes in this band than they have along or farther from the equator. Panel a repre-

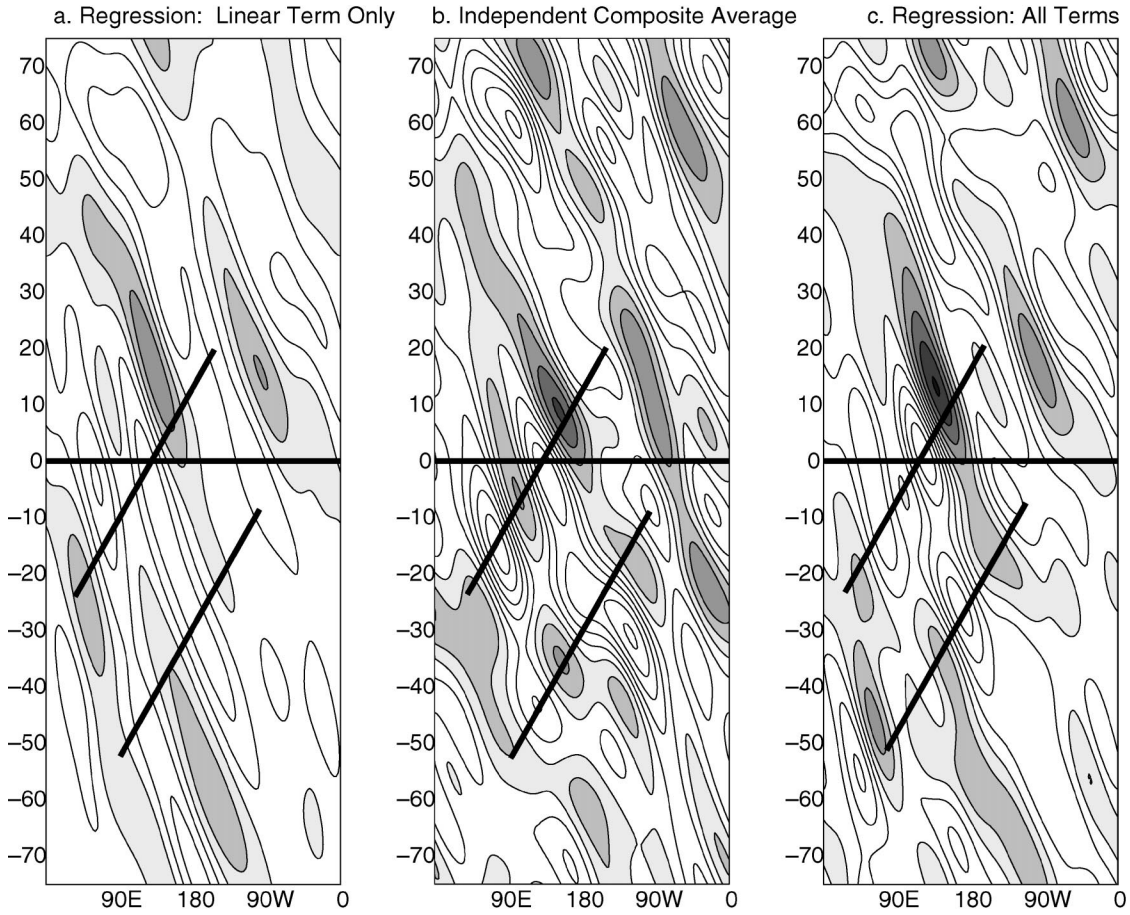

FIG. 1. Longitude–time lag representations of regressed or composited ISOw bandpass-filtered precipitable water anomaly, averaged from 2.5° to 7.5°N. The contour intervals are 0.5 mm of PW, with the first positive contour at 0.25 mm. Positive anomalies are shaded. (a) Regression results for the linear term only. (b) The independent composite average. (c) The full regression model including the linear and nonlinear terms. The thick slanted lines drawn in (a)–(c) approximately trace the locations of local extrema of successive anomalies in (b) and (c) and are included to emphasize the differences between (b) and (c).

sents only the portion of the ISOw PW anomaly that is linearly correlated with the base-point OLR. The composite analysis of panel b is assumed to be a rough approximation of the total part of the ISOw field that is related to the ISOe index series. The main weakness of this composite is that it is sensitive to the criteria used to select the dates over which the ISOw fields are averaged, and that it is based only on one specific point in the wave cycle in the index series. The advantage of panel b is that it includes the responses to both linear and nonlinear interactions between the ISOe and the ISOw.

Comparison of all three panels reveals that the results of the simple composite (panel b) are clearly more similar to the results of the regression model with nonlinear terms (panel c) than to the results of the fully linear regression model (panel a). For example, the highest-amplitude anomalies in both panels b and c cluster along the solid black lines drawn on the diagrams. Such clustering is not as apparent in panel a. We may therefore conclude that the regression model based on the linear term alone is leaving out part of the relevant ISOw PW signal. The similarities between panels b and c show that addition of the nonlinear terms effectively diagnoses much more of the total ISOw signal that is related to the ISOe index.

It is important to note that we do not expect panels b and c to be identical. Panel c is calculated from a regression relationship that is trained by all of the data in the index series, after eliminating periods when the signal was not deemed to be present. Panel b was calculated from a set of dates that were selected based on a subjective set of criterion applied to the ISOe index series. Nevertheless, this comparison provides evidence that the basic patterns seen in panel c are easily discerned in the data and are not generated by the model form. Among the two regression model results, Panel c is clearly a more complete representation of the portion of the ISOw PW anomalies that are related to the ISOe index than is panel a.

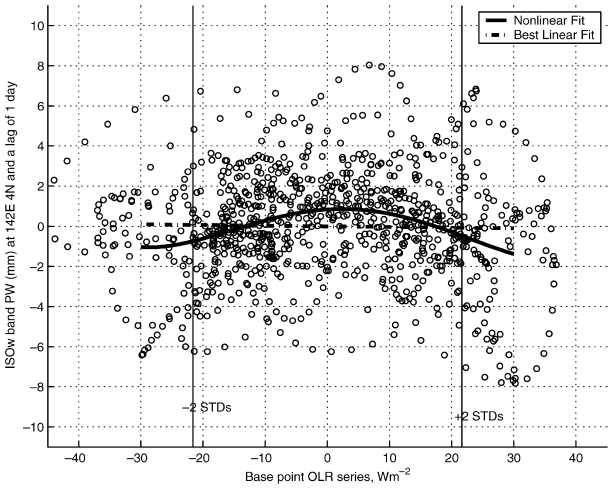

FIG. 2. Scatterplot of ISOw band PW at 4°N, 142°E and a lag of +1 day against the base-point OLR index time series discussed in the text. Only those points that occurred when the index time series was deemed to be active (as discussed in the text) are plotted. The heavy broken line represents the best linear fit, and the heavy solid curve represents fit of the model that includes the linear and three nonlinear terms.

b. Statistics of the model

The independent composite (Fig. 1b) demonstrates that the multiple linear regression model [Eq. (1)] applied to the relationship between the ISOe and the ISOw describes processes that are found in the data rather than processes that are generated by the model itself. The higher-power terms were included in the model because they improve the model fit to the data. The easiest way to show this is by utilizing an example scatterplot of one of the modeled PW time series against the index ISOe OLR series. Figure 2 gives one such example, for ISOw PW anomalies at 4°N, 142°E. Though the relationship for this case is obviously far from perfect, it is clearly more like the curve that includes the nonlinear terms (solid curve) than it is like the dashed line that represents the weak first-order relationship. A linear term alone is clearly insufficient to model this relationship. We calculated the mean square of the model residuals (r^2) for this example, and found to what extent it falls off incrementally when each power term is cumulatively added to the linear model one at a time. The results are shown in Table 1.

If the coefficients assigned to the nonlinear terms are significantly different from zero, then they should not be rejected as describing part of the relationships between the ISOe and the ISOw. The statistical significance of the coefficients associated with these terms is easy to assess. We applied a bootstrap significance test (e.g., Wilks 1995) to determine whether the regression coefficients that generate the solid curve in Fig. 2 are significantly different from zero. This was done by randomly resampling (with replacement) the data from

TABLE 1. Statistics for fit of the model shown in Fig. 2.

Highest power included	r^2 (mm^2)	Probability that coefficients are significantly different from zero
1	7.51	95%
2	7.24	98%
3	7.12	70%
4	7.02	99%

which the coefficients were calculated 10 000 times to find a sample distribution of each coefficient.

This significance test was then extended across the Tropics to include every grid point at the zero time lag in order to show whether each coefficient is significant across the global Tropics. Results for the case shown in Fig. 2 are given in the right column of Table 1. All but the cubic term can be considered significant for this case. Results of the global extended analysis are shown in Fig. 3. Figure 3 shows that all four terms (linear, quadratic, cubic, and quartic) exceed the 99% level over broad regions of the globe. Figure 4 shows how many terms are significant across the global grid at zero lag. In general, regions where none of the terms are found to be significant have anomaly amplitudes that are near zero. The spatial coverage of high significance decreases as the power of the term increases. Figure 3c shows that the case given in Fig. 2 (4°N, 142°E) is located near a local minimum of significance of the cubic term. It also shows that broad regions of high significance levels of the cubic term surround this location. The relationship at this point appears to be nearly symmetric about the zero of the base index. This symmetric pattern indicates that at this lag and location, when the predictor variable is far from zero and of either sign, the dependent variable is more likely to have a negative anomaly than a positive one and, when the predictor anomaly is near zero, the predictand tends to be positive. Figure 2 also hints that, as the low-frequency predictor goes through one cycle (positive to negative and back to positive), the predictand would go through two, by crossing the zero line four times along the regressed curve. This interpretation is not complete, however, because the regression coefficients change with time lag. In any case, the symmetric pattern seen in Fig. 2 cannot be described by a cubic term. However, the cubic term does help improve the phase relationship with the base index at locations where its coefficient is found to be significant.

The analysis of RF also includes a significance test applied to determine whether the composite anomalies themselves were significantly different from zero. They found significant PW anomalies throughout the Tropics at locations far from the base point and at time lags of up to greater than 50 days. Use of PW data results in the higher significance levels attained in the Western Hemisphere than are obtained there by using OLR data (see RF). In addition to the geographical enhancement obtained by using PW, our composites are also enhanced

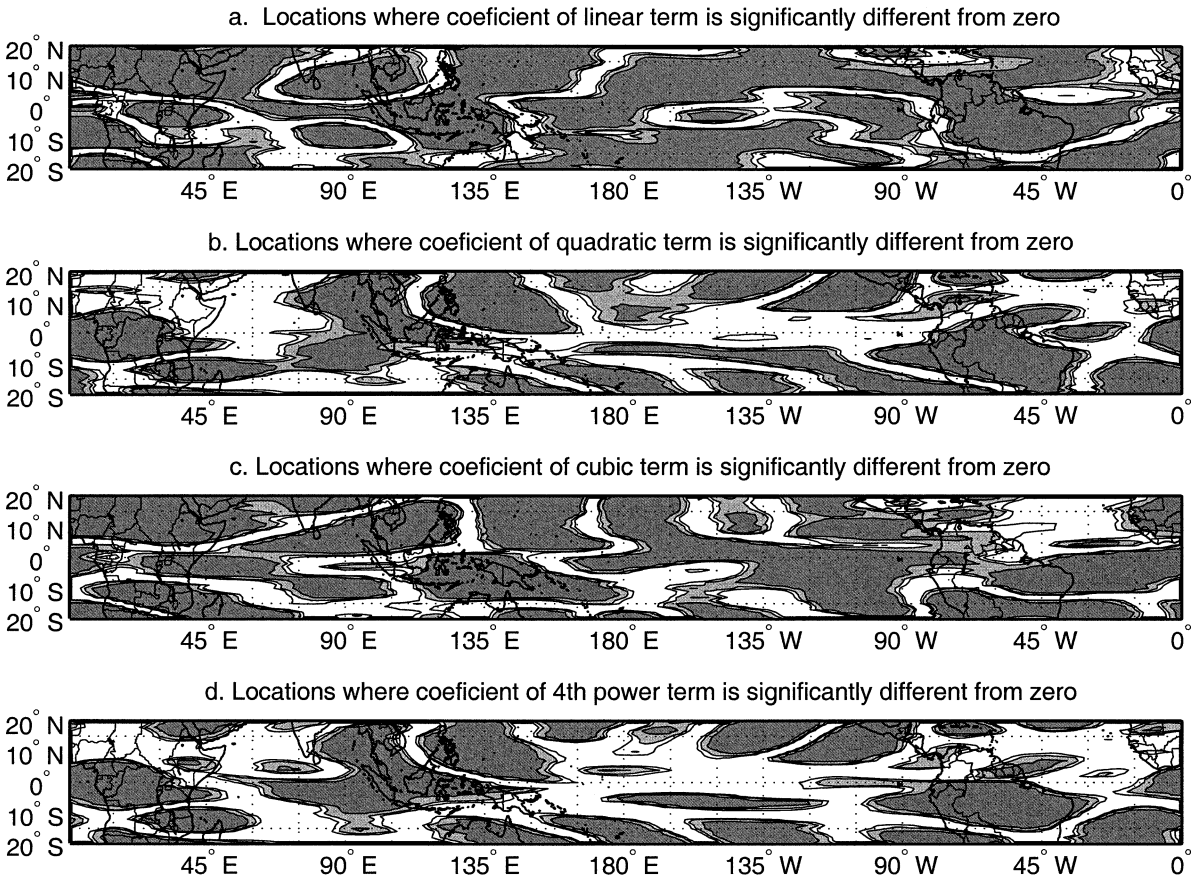

FIG. 3. Geographical locations at which the regression coefficients are significantly different from zero. The 90%, 95%, and 99% levels are plotted, and the darkest shading represents regions where the 99% level is exceeded. (a) The results for the linear term, (b) for the quadratic term, (c) for the cubic term, and (d) for the fourth power term.

at high lags, allowing them to include multiple complete cycles. RF shows that this enhancement results from emphasis on the Southern Hemisphere warm season. Composites based on the entire year (e.g., Hendon and Salby 1994) include only one significant cycle because the differences between the northern and southern summer ISOs cause the composite anomalies containing them both to decay quickly beyond one cycle.

c. Contribution of the nonlinear terms

A discussion of this statistical model would be incomplete without a comparison between the contributions of the linear term and the contributions of the set of nonlinear terms. Figure 5 is included to facilitate this discussion. Figure 5 is a longitude–time lag representation of the PW anomalies contributed by the nonlinear terms and was calculated by finding the differences between Figs. 1a and 1c. Trajectories of regressed ISOe PW anomalies are overlaid on Fig. 5 from Fig. 1a of RF to demonstrate that the nonlinear terms track local interactions between the ISOe and the ISOw.

Figure 5 indicates that the nonlinear terms in our model simulate the nonlinear interactions by which the ISOe modulates the ISOw in regions where ISOe convection is active. This interpretation can be inferred from Fig. 5 because it shows that the nonlinear terms contribute predominantly along trajectories of positive ISOe PW anomalies (approximated by the solid black curves). This argument is supported by the anomalies in Fig. 5 because they tend to have much higher amplitudes and variance along the solid trajectories, whereas they contribute little along the trajectories of negative ISOe PW anomalies (dashed curves).

d. Effect of collinearities

It is possible that collinearities, or correlations between predictor variables, may have large impacts on the results of a multiple linear regression model. These impacts come from the sensitivity of results to the inverse of the matrix $\mathbf{P} = \mathbf{X}^T\mathbf{X}$ in Eq. (3). If $\mathbf{P}$ is close to singular, results may be adversely affected, in part because of round-off errors that prevent the inverse from being correctly resolved (Draper and Smith 1966). Additionally, when $\mathbf{P}$ is close to singular, results become more sensitive to noise in the columns of $\mathbf{X}$. We found that $\mathbf{P}$ is easily invertible on our computer because its

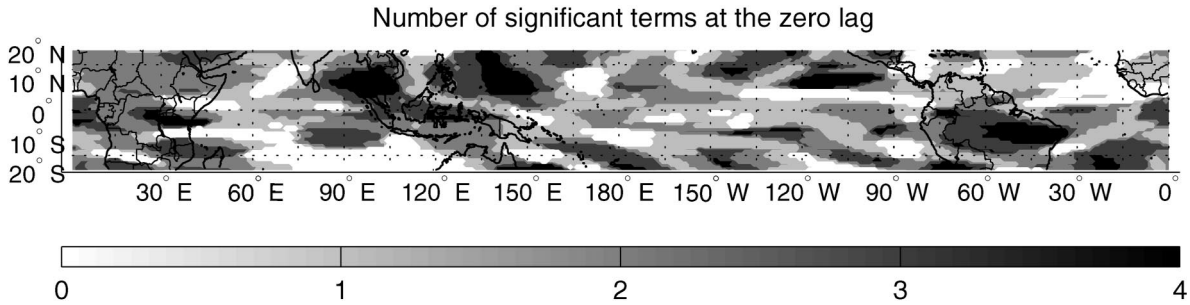

FIG. 4. The number of terms (linear through quartic) found to be significant at above the 99% level at zero lag.

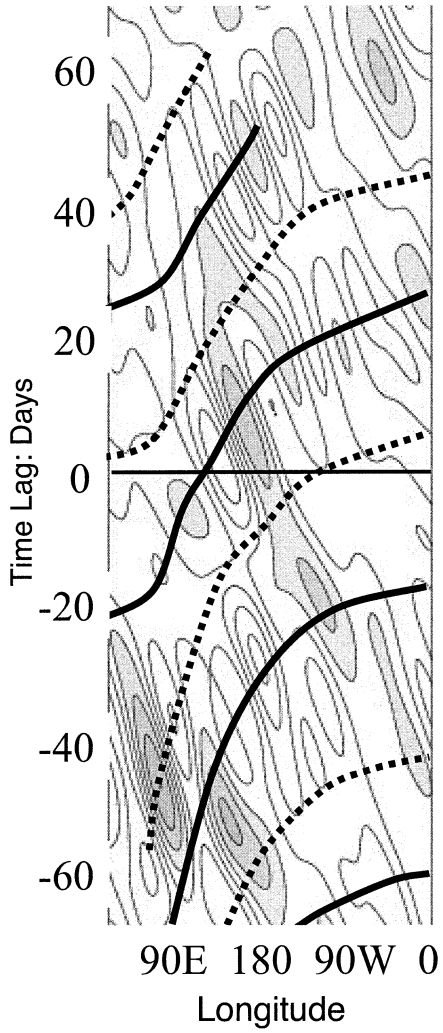

FIG. 5. Longitude–time lag representation of the regressed ISOw band PW anomalies that are contributed by the three nonlinear terms, averaged from 2.5° to 7.5°N. The contour interval is 0.5 mm, and positive anomalies are shaded. Heavy curves superimposed on the diagram are trajectories of regressed ISOe band PW anomalies from Fig. 4a of RF. The solid curves track positive ISOe PW anomalies and the dashed curves track negative ones. The dashed vertical lines mark the locations of the coasts of East Africa and western South America.

floating-point accuracy is more than five orders of magnitude better than needed to be to resolve this inverse. This implies that round-off errors should not contribute significantly to our result. Nevertheless, it is useful to estimate the magnitude of the total effect of collinearities on the results. We did this estimation for our model by calculating the linear projections of the lower-order terms onto the higher-order terms and by iteratively subtracting these projections from the appropriate higher-power terms by applying the Graham–Schmidt process.

The Gram–Schmidt process (e.g., Lay 1994; Draper and Smith 1966, section 5.6) is a well-established method of generating an orthogonal basis that spans the space of the original set of predictors. After applying this process, the resulting set of predictors is orthogonal. After finding an orthogonal basis for the set of predictors, we redid the regression analysis and calculated a new set of composites. The results (not shown) are nearly identical to the original ones, except that the amplitudes of the ISOw PW anomalies are slightly stronger than in the original result. The maximum amplitude adjustment was less than 0.09 mm of PW, or about 2% of the local amplitude. This small improvement does not merit the added complexity of modifying the model by removing all correlations. These results show that collinearities are not responsible for our regression model results and that they can be ignored in this particular application of the model. This test for strong impacts of collinearity should be applied whenever this model form is used, and, if necessary, an orthogonal basis should be used in place of the original set of predictors.

5. Conclusions

The multiple linear regression model described in this paper and applied in RF produces physically valid analyses that reveal processes of partly nonlinear wave interactions that occur in the real tropical atmosphere. These relationships are also visible in a composite average of ISOw bandpass-filtered PW anomalies that is based only on a set of dates of active ISOe convective anomalies at a base point. For this case, the inclusion of the nonlinear terms in the regression improves the resolution of wave interactions relative to a purely linear version of the model.

The regression coefficients of the multiple linear regression model are significantly different from zero across broad regions of the global Tropics, suggesting that the nonlinear model should be applicable throughout the tropical atmosphere. Correlations between the set of predictor variables do not significantly influence the model results for the case analyzed here. However, caution should be applied whenever using this model form because in some cases such correlations could be strong enough to cause the model to distort the image of the processes that the models are designed to diagnose.

Acknowledgments. This work was funded by grants from the National Science Foundation, ATM 0003351 and ATM 0233881, and by a supplemental fellowship from the NASA Pennsylvania Spacegrant Consortium. Dr. George Kiladis offered some additional feedback.

REFERENCES

Dickinson, M., and J. Molinari, 2002: Mixed Rossby gravity waves and western Pacific tropical cyclogenesis. Part I: Synoptic evolution. *J. Atmos. Sci.,* **59,** 2183–2196.

Draper, N. R., and H. Smith, 1966: *Applied Regression Analysis.* John Wiley & Sons, 407 pp.

Hendon, H. H., and M. L. Salby, 1994: The life cycle of the Madden–Julian oscillation. *J. Atmos. Sci.,* **51,** 2225–2237.

——, B. Liebmann, and J. D. Glick, 1998: Oceanic Kelvin waves and the Madden–Julian oscillation. *J. Atmos. Sci.,* **55,** 88–101.

Kessler, W. S., 2001: EOF representations of the Madden–Julian oscillation and its connection with ENSO. *J. Climate,* **14,** 3055–3061.

——, and R. Kleeman, 2000: Rectification of the Madden–Julian oscillation into the ENSO cycle. *J. Climate,* **13,** 3560–3575.

Lay, D. C., 1994: *Linear Algebra and its Applications.* Addison-Wesley, 506 pp.

Liebmann, B., and C. A. Smith, 1996: Description of a complete (interpolated) outgoing longwave radiation dataset. *Bull. Amer. Meteor. Soc.,* **77,** 1275–1277.

Madden, R. A., and P. R. Julian, 1994: Observations of the 40–50-day tropical oscillation—A review. *Mon. Wea. Rev.,* **122,** 814–837.

Randel, D. L., T. H. vonder Haar, M. A. Ringerud, G. L. Stephens, T. J. Greenwald, and C. L. Combs, 1996: A new global water vapor dataset. *Bull. Amer. Meteor. Soc.,* **77,** 1233–1246.

Roundy, P. E., and W. M. Frank, 2004a: A climatology of waves in the equatorial region. *J. Atmos. Sci.,* **61,** 2105–2132.

——, and ——, 2004b: Effects of low-frequency wave interactions on intraseasonal oscillations. *J. Atmos. Sci.,* **61,** 3025–3040.

Sokal, R. R., and F. J. Rohlf, 1995: *Biometry: The Principles and Practice of Statistics in Biological Research.* 3d ed. W. H. Freeman, 887 pp.

Straub, K. H., and G. N. Kiladis, 2003: Interactions between the boreal summer intraseasonal oscillation and higher-frequency tropical wave activity. *Mon. Wea. Rev.,* **131,** 945–960.

Wheeler, M., and G. N. Kiladis, 1999: Convectively coupled equatorial waves: Analysis of clouds and temperature in the wavenumber-frequency domain. *J. Atmos. Sci.,* **56,** 374–399.

——, ——, and P. J. Webster, 2000: Large-scale dynamical fields associated with convectively coupled equatorial waves. *J. Atmos. Sci.,* **57,** 613–640.

Wilks, D. S., 1995: *Statistical Methods in the Atmospheric Sciences: An Introduction.* International Geophysical Series, Vol. 59, Academic Press, 467 pp.